

# Numerical Simulation of Combustion Processes in a Gas Turbine

Authors: György Bicsák<sup>[1]</sup>, Anita Hornyák<sup>[2]</sup> and Dr. Árpád Veress<sup>[3]</sup>

<sup>[1]</sup> PhD Student, Budapest University of Technology and Economics, Department of Aircraft and Ships, Sztoczek u. 6. J. ép. 418, Budapest H-1111, Hungary, e-mail: gybicsak@rht.bme.hu, phone: + 36-1-463-1867

<sup>[2]</sup> Development Engineer, Knorr-Bremse Sfs, H-1238, Budapest, Helsinki út 105, Hungary, e-mail: anita.hornyak@knorr-bremse.com, phone: + 36-1-28-94-655

<sup>[3]</sup> Associate Professor, Budapest University of Technology and Economics, Department of Aircraft and Ships, Sztoczek u. 6. J. ép. 426, Budapest H-1111, Hungary, e-mail: averess@rht.bme.hu, phone: + 36-1-463-1992

**Abstract:** The type of the fuel, upstream and downstream flow conditions, fuel injection and mixing processes together with the geometry of the combustion chamber have a significant effect on efficiency, power, fuel consumption, noise and emission of the gas turbines. These contributions can be considered also in the virtual prototyping of combustion chambers, by which significant amount of time, cost and capacity can be saved. However, the accuracy of these approaches must be within 5-10 % for industrial relevancies. Hence, a three dimensional, turbulent flow and gas phase combustion has been modelled in a tubular combustion chamber of a gas turbine with the main goal of comparing the effect of different combustion models and solid wall boundary conditions with real tests. Four combustion models as Eddy Dissipation Model (EDM), Probability Density Function Flamelet Model (PFM), Burning Velocity Model (BVM) and Fluent Non-Premixed Model (FnPM) have been applied beside using k- $\epsilon$  turbulence model in the simulations. Three different incoming mass flows were implemented according to the measurements, which originate from Serag-Eldin and Spalding's paper [1.]. Although natural gas has been used in the real tests, methane combustion has been modelled in the simulations, because the dominant component of the burnt natural gas was methane in 93.63 %. The results were examined in 3 cross sections at certain axial distances along radii. The closest results to the measurements were provided by FnPM, most probably due to the more accurate thermal boundary conditions at the solid walls. In that case, the temperature differences between the measurements and the simulations were within the 30 % error margin in the 100 % of the investigated radius on the average, within 10 % in the 98.6 % and within the 5 % in the 79.1 %.

**Keywords:** CFD; Gas turbine; Combustion Modelling; Eddy Dissipation Model; Probability Density Function Flamelet Model; Burning Velocity Model; Non-Premixed Model

## INTRODUCTION

Nowadays, the only gas turbines have energetical and economical relevancies to be applied in the propulsion system of the commercial aircraft due to their high power density and low range factor<sup>1</sup> at high speed flight below Mach number 1.

Although experience and the know-how of the gas turbine manufacturers have been increasing continuously, the measurement-based development of the parts are long, costly processes and it requires considerable amount of capacity. However, due to the fast developments of the computer technology and the tools in CAD (Computer Aided Design) systems, these resources can be decreased significantly.

The aircraft are equipped with the high level technology based components, amongst which the combustion chambers are responsible for the most complex physical processes as converting chemical

energy in heat, but the improvements of power, efficiency, heat loading, emissions, noise and the flame-out at critical conditions are still open issues in their design and developments.

Furthermore, as fossil fuels have become more and more expensive and the environmental regulations make new demands for the amount and composition of the exhaust gases, the aeronautical industry has to find new, sustainable solutions for the fuel problem. The implementation of the alternative fuels is time consuming and expensive process, which could be improved by using validated simulation methods.

Hence, as a conclusions of the fore-mentioned issues confirmed by the increasing number of the publication in this area [2-9], three-dimensional multiphysics-based numerical simulations of the combustion processes are going to spread more and more in the development of the gas turbine combustion chambers, because, with this tool, designers can receive information not only about the main characteristics of the combustions, but using a wide range of visualization tools, additional information is available by CFD (Computational Fluid Dynamics) simulations, which otherwise appears only when applying very

---

<sup>1</sup>The range factor, in this manner, is the ratio of the weight of the fuel and engine to the engine net thrust decreased by the nacelle drag for a range and flight speed [18].

complex and expensive laser diagnostics to a dedicated research of the combustion chamber that was modified for optical access.

However, the development of adequate and accurate CFD methodology and the efficient computer codes for combustion simulation with acceptable time-consumption are still challenging task [17]. The solution of the compressible multiphase or multi-component turbulent flow must be calculated together with heat transfer and different chemical reactions, which requires additional equations beside the Navier-Stokes and turbulence modelling for reaction kinetics, injection, atomization, ignition and formation of exhaust gases for example.

The main goal of the present article is to compare the accuracy of different combustion models and thermal wall boundary conditions with measurements and determine their industrial relevance's.

## FUNDAMENTALS OF COMBUSTION MODELLING AND GOVERNING EQUATIONS

In CFD, to describe the compressible flow accurately, the pressure ( $p$ ), temperature ( $T$ ), density ( $\rho$ ), velocity vector ( $v$ ) and its components ( $u_x, u_y, u_z$ ) must be well-known in the computational domain, just like the concentration of the mass fraction of each species ( $w_i$ ). Besides the conservation equations (mass, momentum and energy), extra information is given by the reaction kinetic equations for the combustion process.

In the applied approximation, in a laminar flame, the pressure is constant ( $p=const.$ ). The velocity components can be computed from the equation of mass conservation in stationary case [15]:

$$\frac{\partial \rho}{\partial t} + \frac{\partial(\rho v)}{\partial z} = 0 \rightarrow \frac{\partial(\rho v)}{\partial z} = 0 \rightarrow \rho v = const. \quad (1)$$

In the continuity equation of mass fraction of species  $i$ , besides the diffusion and flow component, the chemistry part take role too [15]:

$$\rho \frac{\partial w_i}{\partial t} = \frac{\partial}{\partial z} \left( D_i \rho \frac{\partial w_i}{\partial z} \right) - \rho v \frac{\partial w_i}{\partial z} + r_i \quad (2)$$

where the mass fraction of species  $i$  ( $w_i$ ) can be calculated, if  $v$  is the velocity of the gas mixture,  $D_i$  is the diffusion coefficient and  $r_i$  is the reaction rate, which is defined by the following equation [15]:

$$r_i = M_i \sum_k r_{i,k} = M_i \left( F_k \prod_i c_i^{\eta_{i,k}} - B_k \prod_i c_i^{\eta_{i,k}} \right), \quad (3)$$

$M_i$  is the molar mass,  $c_i$  is the concentration, and  $\eta_{i,k}$  is an exponential index.  $F_k$  and  $B_k$  are the reaction rate constants for reversible and

irreversible processes, and can be determined by the Arrhenius equation [15]:

$$F_k = A_k T^{\beta_k} e^{\left(\frac{-E_k}{RT}\right)}; B_k = F_k T^{\beta_k} e^{\left(\frac{-E_k}{RT}\right)} \quad (4)$$

The  $A_k$  is pre-exponent coefficient,  $E_k$  marks the activation energy,  $R$  is the spec. gas constant, and  $\beta_k$  is the temperature exponent (it's generally 0).

The temperature can be derived from the conservation equation of energy, which is also extended by the chemistry part:

$$\rho c_p \frac{\partial T}{\partial t} = \frac{\partial}{\partial z} \left( \lambda \frac{\partial T}{\partial z} \right) - \sum_i h_i r_i - \left( \rho v c_p + \sum_i j_i c_{pi} \right) \frac{\partial T}{\partial z}, \quad (5)$$

where  $\lambda$  is the thermal conductivity,  $c_p$  is the specific heat at constant pressure and the diffusion of the gas mixture's towards the centre of gravity is marked by  $j_i$ .

Finally, the density can be determined from the ideal gas equation of state:

$$\frac{p}{\rho} = RT \quad (6)$$

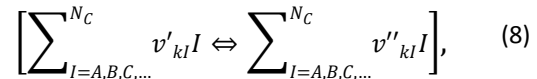
As it was mentioned before, beside the conservation equations, the simulation should be completed by additional models, which can handle the thermochemistry or ignition if it is necessary.

Ansys CFX used combustion models compute the same algorithm, which is used for multi-component fluid, but it is completed with a source/sink term in order to describe the effect chemical reactions. The transport equation for component  $I$  with mass fraction of  $w_I$  is [15]:

$$\frac{\partial(\rho w_I)}{\partial t} + \frac{\partial(\rho u_j w_I)}{\partial x_j} = \frac{\partial}{\partial x_j} \left( \Gamma_{I,eff} \frac{\partial w_I}{\partial x_j} \right) + S_I \quad (7)$$

where  $S_I$  is the source term due to the chemical reaction rate involving component  $I$  and  $\Gamma_{I,eff}$  is effective diffusivity for component  $I$ .

Generally, chemical reactions can be described in terms  $k$  elementary reactions involving  $N_C$  components in the following way [15]:



where  $v_{kl}$  is the stoichiometric coefficient for component  $I$  in the elementary reaction  $k$ .

For  $I$  component, the rate of production/consumption ( $S_I$ ) is calculated by [15]:

$$S_I = W_I \sum_{k=1}^K (v'_{kl} - v''_{kl}) R_k, \quad (9)$$

where  $R_k$  is the elementary reaction rate of progress for reaction  $k$ , which is calculated with Eddy Dissipation Model or/and Finite Rate Chemistry Model in CFX.

The **Eddy Dissipation Model (EDM)** is especially suitable for the chemical reactions, which go through in a short time, and the fluid flow is turbulent and non-premixed. The reagents

mix in molecular level, and transforms into flue immediately. In the case of EDM, the mixing time is influenced by the properties of the vortices. The speeds of the reactions are controlled by the reagents' and flues' concentration and the maximum temperature of the flame. EDM assumes that the chemical reaction is relative fast to the transport processes in the flow. Products are formed instantaneously when the reactants mix at the molecular level. The reaction rate is related to the time required to mix reactants at the molecular level. In the case of turbulent flows, the Eddy properties dominate the mixing time, therefore the rate is proportional to a mixing time defined by the turbulent kinetic energy ( $k$ ), and dissipation rate ( $\varepsilon$ ) [15]. In EDM the progress of elementary reaction  $k$ , is determined by the smallest of the reactants limiter and products limiter. The reactants limiter is given by [15]:

$$R_k = A \frac{\varepsilon}{k} \min \left( \frac{[I]}{v'_{kl}}, \right), \quad (10)$$

where  $[I]$  is the molar concentration of component  $I$  and it includes the reactant components. The products limiter is the following [15]:

$$R_k = A B \frac{\varepsilon}{k} \left( \frac{\sum_P (I) W_I}{\sum_P v''_{kl} W_I} \right) \quad (11)$$

where  $P$  loops over all product components in the elementary reaction  $k$ . If  $B$  coefficient is negative, the product limiter is disabled. The maximum flame temperature limiter is defined by [15]:

$$R_{k,MFT} = A \frac{\varepsilon}{k} C_{MFT}, \text{ where} \quad (12)$$

$$C_{MFT} = \max\{(T_{max} - T), 0[K]\} \cdot \frac{\rho C_p}{\Delta H_R}$$

If the temperature is equal to the maximum flame temperature,  $C_{MFT}$  virtual concentration vanishes.  $\Delta H_R$  marks the reaction heat release per mole [15].

The **PDF Flamelet Model (PFM)** can be used, if the flow is turbulent, the Damköhler number is much greater than 1 and non-premixed combustion is modelled. The Damköhler number is the quotient of the mixing ( $\tau_t$ ) and chemical reaction time ( $\tau_c$ ) [15]:

$$Da = \frac{\tau_t}{\tau_c} \quad (13)$$

The actual combustion goes through in a thin surface, which called flamelet. The model sets up the turbulent flame from laminar flamelets. The PFM doesn't use the transportation equations written to the components, but uses the conservation equations written to the mixture fraction  $Z$ , which is peculiar to the non-premixed models. Chemical reactions not influence the mixture fraction ( $Z$ ), because it deals with elements rather than molecules and elements are not affected by chemistry [15]:

$$\frac{\partial(\rho Z)}{\partial t} + \frac{\partial(\rho Z)}{\partial x_j} = \frac{\partial}{\partial x_j} \left( \rho D \frac{\partial Z}{\partial x_j} \right) \quad (14)$$

The  $Z=Z_{st}$  isosurface determines the stoichiometric mixture.

The most important advantage of the model, that it gives detailed information about the molecular movement process and the elemental chemical kinetics. In the case of short distances, the time is negligible. The method uses pre-calculated models on laminar model flames, which also reduce the time-consumption of the simulation.

The **Burning Velocity Model (BVM)** includes laminar flamelets and additionally to the PDF, the advancement of the reactions. The balance equation is written to the average advancement factor. BVM is used to close the combustion source term ( $\bar{\omega}_c$ ) for reaction progress [15]:

$$\bar{\omega}_c = \bar{S}_c - \frac{\partial}{\partial x_j} \left( (\overline{\rho D}) \frac{\partial \tilde{c}}{\partial x_j} \right) \quad (15)$$

where

$$\bar{S}_c = \bar{\rho}_u S_T |\nabla \tilde{c}| \quad (16)$$

$\bar{\rho}_u$  is the density of the unburnt mixture,  $\bar{S}_c$  is the source term,  $S_T$  is a closure for the turbulent burning velocity,  $\tilde{c}$  is the averaged reaction progress variable. The reaction progress variable is computed from the following transport equation [15]:

$$\frac{\partial(\bar{\rho} \tilde{c})}{\partial t} + \frac{\partial(\bar{\rho} \tilde{u}_j \tilde{c})}{\partial x_j} = \frac{\partial}{\partial x_j} \left[ \left( \overline{\rho D} + \frac{\mu_t}{\sigma_c} \right) \frac{\partial \tilde{c}}{\partial x_j} \right] + \bar{\omega}_c \quad (17)$$

Ansys **Fluent Non-Premixed** model can be used to simulate fast, turbulent reactions, in the case of chemical equilibrium, or laminar flamelet structure. Under the simplification of equal diffusivities, the equations of species can be reduced to a single equation for the mixture fraction,  $f$ .

The reaction source terms in the species equations are neglected, thus the mixture fraction is a conserved quantity. In the case of turbulent flows, the assumption of equal diffusivities is acceptable, where the turbulent convection overwhelms molecular diffusion. The Favre mean (density-averaged) mixture fraction equation is [16]:

$$\frac{\partial}{\partial t} (\bar{\rho} \bar{f}) + \nabla \cdot (\bar{\rho} \vec{v} \bar{f}) = \nabla \cdot \left( \frac{\mu_t}{\sigma_f} \nabla \bar{f} \right) + S_m + S_{user} \quad (18)$$

where  $S_m$  is a source term to describe transfer mass into the gas phase from liquid fuel droplets or reacting particles,  $S_{user}$  is any user-defined source term. Additionally, Ansys Fluent solves a

conservation equation for the mixture fraction variance  $\overline{f'^2}$  [16]:

$$\frac{\partial}{\partial t} (\rho \overline{f'^2}) + \nabla \cdot (\rho \vec{v} \overline{f'^2}) = S_{user} + \nabla \cdot \left( \frac{\mu_t}{\sigma_t} \nabla \overline{f'^2} \right) + C_g \mu_t (\nabla \bar{f})^2 - C_d \frac{\epsilon}{k} \overline{f'^2}, \quad (19)$$

where  $f' = f - \bar{f}$ , the values of constants  $\sigma_t$ ,  $C_g$ , and  $C_d$  are 0.85, 2.86 and 2.0 respectively.

## SIMULATION OF THE COMBUSTION PROCESS

The combustion process was simulated in a 3 dimensional simple tubular combustor. Although this kind of model is not used in the aircraft gas turbines because of its size, geometry and efficiency, it seems to be ideal for comparing the effect of the different reaction models and wall thermal boundary conditions with each other and the measurements at significantly less computational resources; performance requirements and time-consumption.

The base of the comparison of the 4 models (EDM, PFM, BVM, and FnPM) was the calculated and measured temperature distribution along the radius at the certain axial locations. The measured data were adopted from Serag-Eldin and Spalding's article [1]. The difference of the real and the simulated temperature distributions were also compared with each other.

Besides the accuracy, the computational time is also investigated, because one of the other key purposes of this study is to find the model with the reasonable simulation time.

### Geometric Model

The inside diameter of the tubular combustor is 0.21 m and its length is 2 m. The fuel and primary air enters into the chamber separately, in non-premixed form. The gaseous fuel inlet is a spherical tube with 19.5 mm diameter and the primary air enters through a swirler, which is made of 10 vanes with 42.5 mm diameter inside and 78.1 mm diameter outside. The leading edges of the vanes has 45° angle to the axis of the combustor.

The diameters of the dilution bores are 25.4 mm and their axes are 240 mm far from the air and fuel inlet surfaces. The measurements were performed in 3 cross sections (marked as I, II, and III.), 0.04 m, 0.08 m and 0.12 m far from the dilution holes respectively (see Figure 3).

IGES format was used to export CAD model of the combustion chamber (see Figure 1.) into the simulation environment. The flow-field was created in Ansys Design Modeller with the Boolean subtract function.



FIGURE 1: The CAD model of combustion chamber

### Numerical Mesh

The mesh was also created in Ansys environment. Hex-dominant elements could not be used due to the small channels, gaps and bores, hence the mesh was built up from 1,954,035 tetrahedrons and 523,458 nodes. Generally 5.5 mm element-size was used, but adjacent to the inlet surfaces, vane walls and flame front, the mesh was finer for higher resolution. Inflation layers were created along the vanes and walls (see Figure 2.).

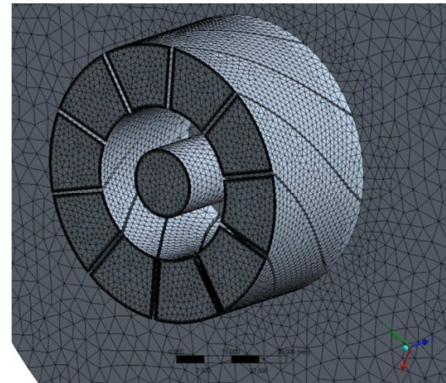


FIGURE 2: The inflation layers in the vanes

### Boundary Conditions

The gaseous fuel consisted of 93.63% methane, 3.25% ethane, 1.78% nitrogen, 0.69% propane and 0.65% other materials [1.]. Concerning the dominant components of the methane, its combustion and so its reaction kinetic equations were used in the simulation. Two material models has been applied, including the following reactions:

@Methane Air WDI NO PDF (EDM):

- *Methane Oxygen WDI*: It is a single-step reaction, which includes the combustion of methane. It is a stoichiometric reaction, the reagents are methane and oxygen and the products are CO<sub>2</sub> and H<sub>2</sub>O. The one-way reaction is solved with the Arrhenius equation.

- *Thermal NO PDF*: includes thermal NO formation in a single-step process. The NO forms

during the reaction of nitrogen and oxygen. The reaction is solved by using the Arrhenius equation completing with the probability density distribution of temperature.

- *Prompt Methane PDF*: includes the NO formation's single step process. During the reaction NO forms from methane, oxygen and nitrogen. The Arrhenius equation is solved also and it is completed with the probability density distribution of temperature.

@Methane Air FLL STP and NO PDF (PFM, BVM):

- *Methane Air FLL STP*: The combustion of the methane is determined by multiple step reaction chain with consisting flamelets. The reagents are the methane and oxygen, but intermediate products form during the process.

- *Thermal NO O Radical PDF*: The formation of thermal nitrogen-oxide is the same, as it was introduced before, but the parameters of the Arrhenius equation are different.

- *Prompt NO Methane PDF*: Consists of the prompt NO formation also in the same way as it was introduced in case of *Methane Air WDI NO PDF* material model.

k-ε turbulence model was used with energy transport equation in the all investigated cases. The reference pressure was 101325 Pa, and P1 model was applied for thermal radiation. The B constant was 0.5 in case of EDM. Ignition model was not used, so the initial temperature was 1300 K to reach the necessary activation energy level. Adiabatic wall was defined in EDM, PFM and BVM, while 570 K average wall-temperatures was imposed – similar to the measurements – at FnPM model at Flame “A”, “B” and “C” cases.

The inlet mass flows at the three different test cases are shown in Table 1.

TABLE 1: Mass flow inlets

Boundary name	Flame „A” [kg/s]	Flame „B” [kg/s]	Flame „C” [kg/s]
Primary air inlet	0.039	0.039	0.0562
Dilution air	0.041	0.061	0.0352
Fuel inlet	0.00155	0.00155	0.00219

## Results

The results were quantitatively analysed in the already mentioned 3 cross sections (I, II, and III) and their intersection with 6 longitudinal planes (1-6) representing 18 lines from the axis to the outer radius of the combustion chamber (see Figure 3 and 7.). Of course, considering the amount of the results, only a few of them is shown in this article. The temperature distributions of the first boundary conditions (Flame “A”) are shown in the next figures (Figures 3-6). Regarding the qualitative results, it can be observed, that the different combustion models can provide relatively large

differences in temperature distribution resulted by the different wall thermal boundary conditions and other physical and mathematical approaches implemented in the models.

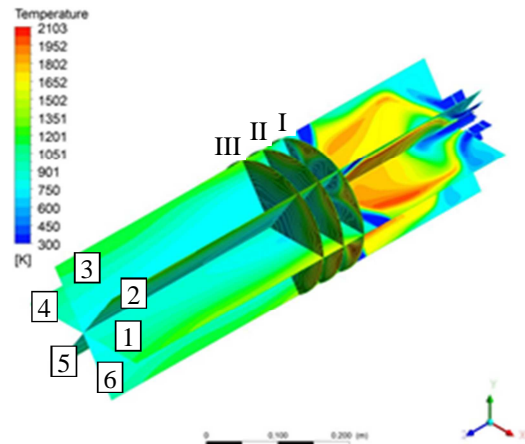


FIGURE 3: The temperature distribution with EDM model (Flame „A”)

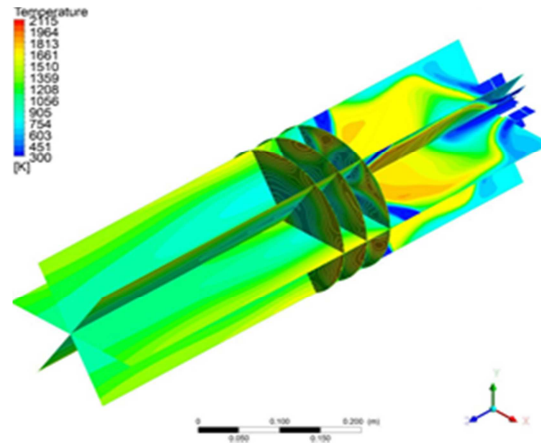
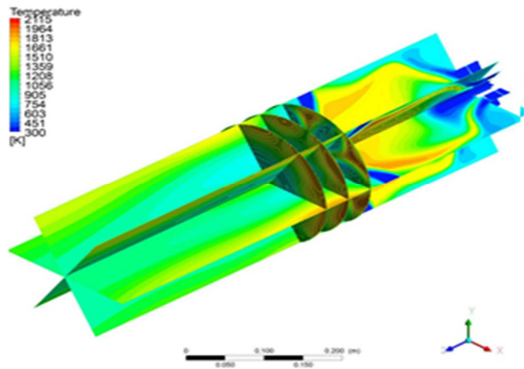


FIGURE 4: The temperature distribution with PFM model (Flame „A”)

As the figures show, the cold gaseous fuel and primary air enters into the chamber across the swirling vanes, they mix due to the recirculating and swirling flow and when the mixture reaches the activation conditions, the flame front forms. The maximum temperature is the same in the case of PFM and BVM models (2115 K), they are close to EDM model (2103 K), and they are higher with 12 % than the results of the Fluent non-premixed model (1886 K). Close to the dilution bores, the entering cold air mixes with the burnt and unburnt particles, hence the temperature of the mixture decreases. In case of CFX models, close to the walls, behind the dilution bores the temperature is higher due to the adiabatic wall conditions and the reignitions of the mixture. This phenomenon decreases the accuracy of the model and it should be avoided by using more realistic boundary conditions at that area.

The computed temperature results of the 4 reaction models were compared to the measured



**FIGURE 5:** The temperature distribution with BVM model (Flame „A”)

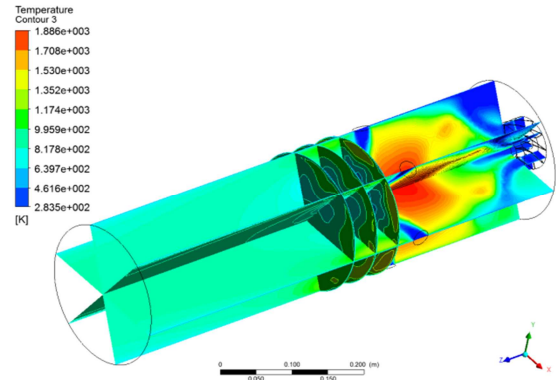


**FIGURE 6:** The temperature distribution with Fluent non premixed model (Flame „A”)

data along the intersecting radius of the 6<sup>th</sup> plane and I, II and III cross sections (see Figure 3. and 7.). The differences between the results and the

measurements were calculated in the percent of the measured values (see Table 2.), grouped in the 5, 10 and 30 % deviation margin and expressed in the function of the radius %.

**TABLE 2:** Accuracy of the simulations along the investigated radius within the given deviation margin expressed in the radius %

		Eddy Dissipation Model		PDF Flamelet Model		Burning Velocity Model		Ansys Fluent Non-premixed Model		
Deviation [%]		<10%	<30%	<10%	<30%	<10%	<30%	<10%	<30%	<5%
Flame "A"	I.	42	81	51	67	48	76	100	100	84
	II.	37	70	31	100	58	100	96	100	52
	III.	30	70	31	95	47	100	95	100	73
Flame "B"	I.	84	99	71	100	54	100	96	100	72
	II.	47	99	46	98	43	79	100	100	84
	III.	29	93	50	95	46	75	100	100	97
Flame "C"	I.	5	87	7	90	10	91	100	100	86
	II.	51	100	42	100	25	100	100	100	84
	III.	50	84	35	91	39	76	100	100	80
<b>Average:</b>		41.6	87	40.3	92.9	41.1	88.6	98.6	100	79.1

The temperature results in the investigated cases were deviated from the measurement (see Figure 7 and 8.) with different extent. For example, in case of Eddy Dissipation Model at Flame "A" boundary condition in the I<sup>st</sup> cross section along the investigated radius, the temperature differences between the simulation results and the measurement was less than 10% in the 42% of the investigated radius. Similarly, the temperature deviation in the 81 % of the radius was within the 30 % error margin. It can be also observed that the Eddy Dissipation, PDF Flamelet and Burning Velocity Models provide similar results on the average.

The most accurate results were computed by the Fluent non-premixed model. As Table 2, Figure 7. and 8. represent, the temperatures along the 100% of the investigated radius were within the 30% error margin compared with the measurement. Moreover, temperatures deviation, on the average, at 98.6% of the radius was within the 10% error margin and only 20.9% showed larger deviation than 5%.

The differences between the measured and computed results can be caused by several reasons. Regarding the simulations, the deviations can be caused by the different boundary conditions

applied for the bounding walls and the simplifications accompanying with the numerical simulations. It must be considered also that the results are depends on the mesh resolution and so the mesh sensitivity analyses are indispensable to have.

The difference between the time-consumptions of the steady state calculations is conspicuous. The iteration numbers, under which the residuals become converged, were different. In case of EDM, more than 1000 iterations were necessary. This number at the models using flamelets (PFM, BVM) was lower, while in case of Fluent non-premixed model 200 iterations was enough to reach the convergence criteria. The time consumption was correlated with the iteration numbers. The computational time was around 40 hours in the case of EDM, 20-30 hours at flamelet-based models and 3 hours at the Fluent non-premixed model.

Transient simulation was performed also in case of BVM to recover the effect of unsteadiness. Concerning the results at the present case, it can be concluded that if the combustion process is not disturbed and its structure doesn't change, the application of the transient solver is not necessary. However, the time dependence can be important in

the case of ignition, start-up process, flame-out, or

when the mass flow of the reagents changes.

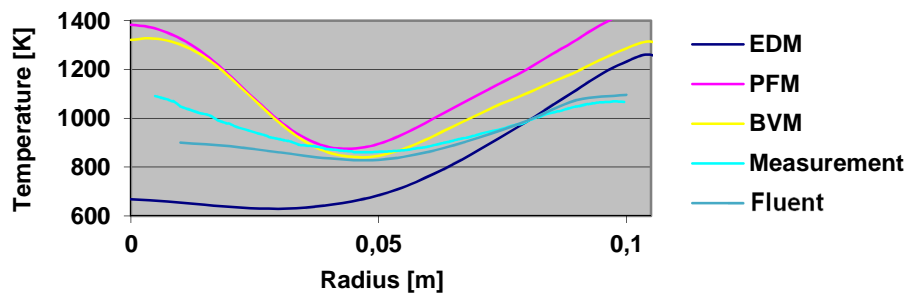


FIGURE 7: The computed and measured temperature distribution along the radius at the intersection of planes 6<sup>th</sup> and III. (Flame „A”)

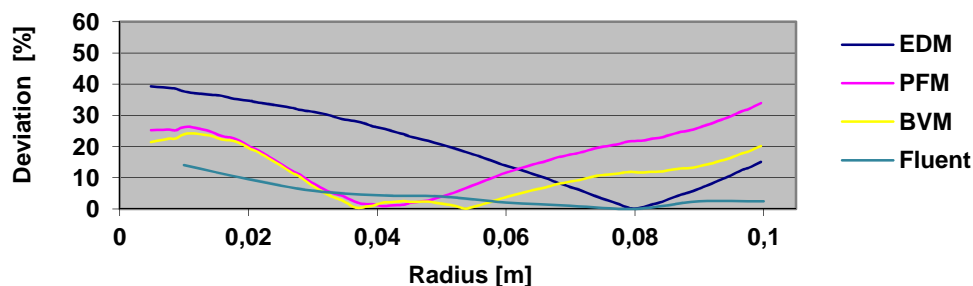


FIGURE 8: Deviation of temperature values from the measurement along the radius at the intersection of planes 6<sup>th</sup> and III. (Flame „A”)

## CONCLUSIONS

The main goal of the present article is to compare the effect of different combustion models and wall thermal boundary conditions with real tests. Four combustion models as one volumetric (EDM in CFX), two flamelet-based (PFM and BVM in CFX) and one mixture fraction-based non-premixed model (in Fluent) have been applied beside using  $k-\epsilon$  turbulence model in the simulations. Three different mass flows as inlet boundary conditions were implemented in correlation with the measurements, which are originated from the Serag-Eldin and Spalding’s paper [1.]. The same geometry and similar material properties were used in the numerical modelling than in [1.].

Concerning the results of the simulations in case of EDM, PFM and BVM, the temperature differences between the analyses and the measurements, on the average, in the 90% of the investigated radii were within the 30 % error margin and in the 40 % were within the 10 %. The origin of this significant deviation can be caused by the adiabatic wall boundary conditions. The EDM, PFM and BVM models provide approximately similar results with each other on the average. The most accurate results were obtained by Ansys Fluent non-premixed model, in which, the temperature differences between the measurements and the simulations were within the 30 % error margin in the 100 % of the investigated radius on the average, within 10 % error margin in

the 98.6 % and within the 5 % in the 79.1 %. However, instead of adiabatic condition, specific wall temperature has been used in those models.

Additionally, the time-consumption of the Fluent non-premixed model was nearly 10 times less than the other models.

Of course further validations are necessary to be completed with mesh-size sensitivity analyses on different geometries and boundary conditions with especially care for investigating the mass fraction of the exhaust gases.

The calculation method can be used in the combustion chamber design only the case, when the 100 % of the computed results (temperature, pressure, density, velocity components, mass fraction of species) will be within the 5-10% error margin with reasonable computational time and resources.

The presented CFD based computational approaches can strongly contribute to improve the performance, efficiency and emissions of the combustion chambers beside allowing possibilities for investigating the effect of alternative fuels concerning the expected goals and taking care for the requirements and standards.

## ACKNOWLEDGEMENT

The work reported in the paper has been developed in the framework of the project "Talent care and cultivation in the scientific workshops of BME" project. This project is supported by the grant \*/TÁMOP - 4.2.2.B-10/1--2010-0009/\*

## NOMENCLATURE

$A_k$	pre-exponent coefficient
$B_k, F_k$	reaction rate constants for reversible and irreversible process
$c_i$	concentration of species $i$
$c_p$	heat capacity
$\tilde{c}$	averaged reaction progress variable
$C_g, C_d$	constants
$Da$	Damköhler number
$D_i$	diffusion coefficient of species $i$
$E_k$	activation energy
$[I]$	molar concentration of component $I$
$\tilde{j}_i$	diffusion of the gas mixture's towards the centre of gravity
$k$	turbulent kinetic energy
$M_i$	molar mass of species $i$
$p$	pressure
$r_i$	reaction rate of species $i$
$R$	gas constant
$R_k$	elementary reaction rate; reactants limiter; product limiter
$R_{k,MFT}$	maximum flame temperature limiter
$\bar{S}_c$	source term
$S_I$	rate of production/consumption
$S_m$	source term to describe mass transfer from liquid fuel droplets to gas phase
$S_T$	closure for the turbulent burning
velocity	
$S_{user}$	user defined source term
$t$	time
$T$	temperature
$v, u_x, u_y, u_z$	velocity vector
$v_{kl}$	stoichiometric coefficient
$w_i$	mass fraction of specie $i$
$x, y, z$	Descartes coordinates
$Z$	mixture fraction
$\beta_k$	temperature exponent
$\Gamma_{eff}$	effective diffusivity for component $i$
$\varepsilon$	dissipation
$\eta_{i,k}$	exponential index
$\lambda$	thermal conductivity
$\rho$	density
$\bar{\rho}_u$	density of the unburnt mixture
$\sigma_c$	turbulent Schmidt number
$\tau_t$	mixing time
$\tau_c$	chemical reaction time
$\bar{\omega}_c$	combustion source term

## REFERENCES

1. Serag-Eldin, M. A., Spalding, D. B., *Computations of Three-dimensional Gas Turbine Combustion Chamber Flows*, ASME J. Engineering for Power, Vol. 101, pp. 326-336, 1979.
2. Ghenai C., *Combustion of Syngas Fuel in Gas Turbine Can Combustor*, Advances in Mechanical Engineering, Volume 2010, Article ID 342357, 2010.
3. N. T. Weiland, C. R. Bedick, P. A. Strakey, *Stability, Emissions, and Boundary Conditions for a Model Validation Combustor*, Spring Technical Meeting of

- the Central States Section of the Combustion Institute,  
[https://www.combustioninstitute.org/upload\\_resources/12S-109.pdf](https://www.combustioninstitute.org/upload_resources/12S-109.pdf), April 22-24, 2012.
4. M. Kanniche, *Modelling Natural Gas Combustion in Gas Turbine: Coupling 3D Combustion Simulations with Chemical Reactor Network for Advanced NOx Prediction*, Chemical Engineering Transactions, Volume 18, ISBN 978-88-95608-04-4, ISSN 1974-9791, 2009.
  5. L. de O. Rodrigues, Marco Antônio Rosa do Nascimento, *Pre-mixed and Diffusion Flames Assessment Using CFD Tool for Natural Gas and Biogas Fuels in Gas Turbine Combustion Chambers*, WSEAS Transactions on Fluid Mechanics, Issue 2 Volume 4, ISSN: 1790-5087, 2009.
  6. H-J. Tomczak, G. Benelli, L. Carrai, D. Cecchini, *Investigation of a Gas Turbine Combustion System Fired with Mixtures of Natural Gas and Hydrogen*, IRFR Combustion Journal, Article Number 200207, ISSN 1562-479X, 2002.
  7. S. Khayamyan, *Flow Field in a Gas Turbine Burner*, MSc thesis, Luleå University of Technology, Department of Applied Physics and Mechanical Engineering, Division of Fluid Mechanics; ISSN: 1653-0187, <http://epubl.ltu.se/1653-0187/2010/012/LTU-PB-EX-10012-SE.pdf>, 2010.
  8. P. Farries, Chris Evers, *Aviation CO<sub>2</sub> Emissions Abatement Potential from Technology Innovation*, QINETIQ/CON/AP/CR0801111, <http://theccc.org.uk/pdfs/QinetiQ%20aviation%20report%20for%20the%20CCC.pdf>, 2008.
  9. K. M. Saqr, M. A. Wahid, *Comparison of Four Eddy-Viscosity Turbulence Models in the Eddy Dissipation Modelling of Turbulent Diffusion Flames*, Int. J. of Appl. Math and Mech. 7 (19): 1-18, 2011.
  10. J. Warnatz, U. Mass, R.W. Dibble, *Combustion; Physical and Chemical Fundamentals, Modelling and Simulation, Experiments, Pollutant Formation*, ISBN-10 3-540-25992-9 4th ed. Springer Berlin Heidelberg New York, 2006.
  11. K. Saeed, C. R. Stone, *The Modelling of a Premixed Laminar Combustion in a Closed Vessel*, Institute of Physics Publishing, Combustion Theory and Modelling, <http://www.eng.ox.ac.uk/ice/papers/KhizerCombModelling.pdf>, 2004.
  12. J. K. Nieuwenhuizen, J.J.H. Brouwers, *Modelling of Premixed Laminar Flames*, Technische Universiteit Eindhoven, 1992.
  13. Y. Jaluria, Kenneth E. Torrance, *Computational Heat Transfer*, ISBN 0-89116-286-0; Hemisphere Publishing Corp. 1986.
  14. D. A. Anderson, John C. Tannehill, Richard H. Pletcher, *Computational Fluid Mechanics and Heat Transfer*, ISBN 0-07-050328-1, Hemisphere Publishing Corp. 1984.
  15. *Ansys CFX-Solver Theory Guide*; Release 12.0, April 2009.
  16. *Ansys Fluent Theory Guide*; Release 12.0, April 2009.
  17. A. Evlampiev, *Numerical Combustion Modelling for Complex Reaction Systems*, Moscow, ISBN-10:90-386-2719-X; ISBN-13: 978-90-386-2719-9, 2007.
  18. C. Soares, *Gas Turbine: A Handbook of Air, Land, and Sea Applications*, Elsevier Academic Publication Press, ISBN-978-0-7506-7969-5, 2008.